

This article was downloaded by:

On: 14 January 2011

Access details: *Access Details: Free Access*

Publisher *Taylor & Francis*

Informa Ltd Registered in England and Wales Registered Number: 1072954 Registered office: Mortimer House, 37-41 Mortimer Street, London W1T 3JH, UK



Molecular Simulation

Publication details, including instructions for authors and subscription information:

<http://www.informaworld.com/smpp/title~content=t713644482>

Solubility of gases and solvents in silicon polymers: molecular simulation and equation of state modeling

Ioannis G. Economou^a; Zoi A. Makrodimitri^a; Georgios M. Kontogeorgis^b; Amra Tihic^b

^a Molecular Thermodynamics and Modelling of Materials Laboratory, Institute of Physical Chemistry, National Centre for Scientific Research "Demokritos", Attikis, Greece ^b Department of Chemical Engineering, Technical University of Denmark, Lyngby, Denmark

To cite this Article Economou, Ioannis G. , Makrodimitri, Zoi A. , Kontogeorgis, Georgios M. and Tihic, Amra(2007) 'Solubility of gases and solvents in silicon polymers: molecular simulation and equation of state modeling', *Molecular Simulation*, 33: 9, 851 — 860

To link to this Article: DOI: 10.1080/08927020701280688

URL: <http://dx.doi.org/10.1080/08927020701280688>

PLEASE SCROLL DOWN FOR ARTICLE

Full terms and conditions of use: <http://www.informaworld.com/terms-and-conditions-of-access.pdf>

This article may be used for research, teaching and private study purposes. Any substantial or systematic reproduction, re-distribution, re-selling, loan or sub-licensing, systematic supply or distribution in any form to anyone is expressly forbidden.

The publisher does not give any warranty express or implied or make any representation that the contents will be complete or accurate or up to date. The accuracy of any instructions, formulae and drug doses should be independently verified with primary sources. The publisher shall not be liable for any loss, actions, claims, proceedings, demand or costs or damages whatsoever or howsoever caused arising directly or indirectly in connection with or arising out of the use of this material.

Solubility of gases and solvents in silicon polymers: molecular simulation and equation of state modeling

IOANNIS G. ECONOMOU^{†‡*}, ZOI A. MAKRODIMITRI[†], GEORGIOS M. KONTOGEORGIS[‡] and AMRA TIHIC[‡]

[†]Molecular Thermodynamics and Modelling of Materials Laboratory, Institute of Physical Chemistry, National Centre for Scientific Research “Demokritos”, GR-153 10 Aghia Paraskevi, Attikis, Greece

[‡]Department of Chemical Engineering, Technical University of Denmark, IVC–SEP, DK-2800 Lyngby, Denmark

(Received February 2007; in final form February 2007)

The solubility of *n*-alkanes, perfluoroalkanes, noble gases and light gases in four elastomer polymers containing silicon is examined based on molecular simulation and macroscopic equation of state modelling. Polymer melt samples generated from molecular dynamics (MD) are used for the calculation of gas and solvent solubilities using the test particle insertion method of Widom. Polymer chains are modelled using recently developed realistic atomistic force fields. Calculations are performed at various temperatures and ambient pressure. A crossover in the temperature dependence of solubility as a function of the gas/solvent critical temperature is observed for all polymers. A macroscopic model based on the simplified perturbed chain-statistical associating fluid theory (sPC-SAFT) is used for the prediction and correlation of solubilities in poly(dimethylsilamethylene) and poly(dimethylsiloxane) and also the phase equilibria of these mixtures over a wide composition range. In all cases, the agreement between model predictions/correlations and literature experimental data, when available, is excellent.

Keywords: Silicon polymers; Solubility; Molecular dynamics; Particle insertion; SAFT

1. Introduction

Accurate knowledge of the solubility of gases and solvents in polymers is crucial for the efficient design of industrial processes, as for example a polymer separation process following polymerization reaction, and of novel polymer-based materials, as for example highly pure polymers. Silicon polymers are used widely in many industrial applications including adhesives, coatings, elastomeric seals and membrane materials for gas and liquid separations. In all cases, polymers exist in mixture with one or more solvents.

Gas and solvent solubilities in polymers can be measured experimentally [1], calculated using empirical correlations or models with significant theoretical basis [2]. In recent years, a number of accurate macroscopic models have been proposed for such purposes. Some of the most widely used models include Statistical Associating Fluid Theory (SAFT), Perturbed Chain-SAFT (PC-SAFT) and their various modifications [3–6], and lattice fluid theories [7,8]. Calculations with a simplified PC-SAFT (sPC-SAFT) model will be presented here.

An alternative way to estimate solubility of small molecules in elastomer polymers is through molecular simulation. Advances in applied statistical mechanics and increase of available computing power at relatively low cost have made molecular simulation a powerful tool for this [9]. Polymer molecules and small molecules are modelled using detailed atomistic representation so that simulation results are directly comparable to experimental data [10]. Furthermore, for relatively larger solvent molecules advanced methodologies have been developed for the efficient and accurate estimation of their solubility in polymers [10].

In this work, the solubility of various organic compounds and gases in different silicon containing polymers is calculated using atomistic simulation. Research in “Demokritos” has been directed towards the development of a force-field for silicon polymers able to provide accurate prediction of microscopic structure, thermodynamic and transport properties over a wide temperature and pressure range [11–13]. This force-field is tested here for the prediction of solubility of six *n*-alkanes, four *n*-perfluoroalkanes, five noble gases and

*Corresponding author. Email: economou@chem.demokritos.gr

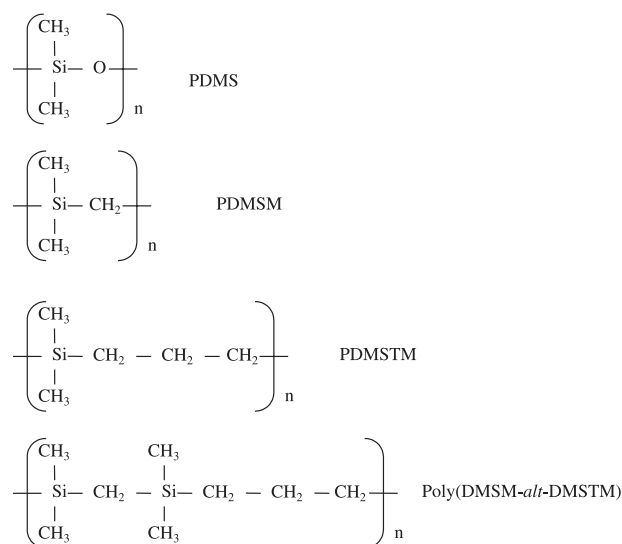


Figure 1. The chemical structure of the silicon polymers examined in this work.

two light gases in poly(dimethylsilamethylene) (PDMSM), poly(dimethylsilatrimethylene) (PDMSTM), their alternating poly(DMSM-*alt*-DMSTM) copolymer and poly(dimethylsiloxane) (PDMS). The chemical structures of the four polymers are shown in figure 1. Solubility of the gas or solvent is calculated using the test molecule insertion method of Widom [14] that is used widely for such calculations.

For many practical applications, reliable fast thermodynamic calculations are required and so molecular simulation becomes impractical. In such a case, an accurate macroscopic model is suitable. In this paper, solubility calculations are presented using the sPC-SAFT model [15,20], a macroscopic model that has been shown to provide accurate description of polymer melt properties. Furthermore, sPC-SAFT is used to predict the phase equilibria of various PDMS-solvent and PDMSM-solvent mixtures. In the case of a macroscopic model, a critical issue is the protocol used for pure component and binary parameter estimation [16]. Some experimental data for the pure polymer melt and for the binary mixture are needed in order to tune model interaction parameters. Here, calculations will be presented for the polymer mixtures where sufficient experimental data are available for reliable parameter estimation. For the case of PDMS mixtures no binary parameter is required while for PDMSM mixtures a small parameter is fitted to experimental binary data. Model calculations are in very good agreement with experimental data in all cases.

2. Atomistic force-field

All of the polymers examined here are flexible polymers consisting of methyl, methylene, silicon and oxygen (in the case of PDMS) atoms or groups. Realistic atomistic force fields for macromolecules account explicitly for the

molecular geometric characteristics as well as for the non-bonded intra- and inter-molecular interactions. In this work, force fields based on the united atom (UA) representation were used. In the UA representation, hydrogen atoms in the methyl and methylene groups are not accounted explicitly, thus reducing the number of “atoms” significantly. Details on the force field development and parameters for the various terms and UAs can be found in Refs. [11–13]. A brief description is given here only.

The potential energy function is written as the sum of contributions due to bond stretching, bond angle bending, dihedral angle torsion and non-bonded interactions between UAs in the same or different chains. In PDMSM, PDMSTM and the copolymer, non-bonded interactions consist of short range van der Waals repulsive and dispersive interactions, while in PDMS long range electrostatic (Coulombic) interactions also exist. The functional form of the force field developed in terms of the potential energy is:

$$\begin{aligned}
 U_{\text{total}}(\mathbf{r}_1, \dots, \mathbf{r}_N) &= U_{\text{stretching}} + U_{\text{bending}} + U_{\text{torsion}} + U_{\text{non-bonded}} \\
 &= \sum_{\text{all bonds}} U(l_i) + \sum_{\text{all bond angles}} U(\theta_i) \\
 &\quad + \sum_{\text{all torsional angles}} U(\phi_i) + \sum_{\text{all pairs}} U(r_{ij}) \\
 &= \sum_{\text{all bonds}} \frac{k_{l_i}}{2} (l_i - l_{i,o})^2 + \sum_{\text{all bond angles}} \frac{k_{\theta_i}}{2} (\theta_i - \theta_{i,o})^2 \\
 &\quad + \sum_{\text{all torsional angles}} \frac{1}{2} k_{\phi} (1 - \cos 3\phi) \\
 &\quad + \sum_{\text{all pairs}} \left(4\epsilon_{ij} \left[\left(\frac{\sigma_{ij}}{r_{ij}} \right)^{12} - \left(\frac{\sigma_{ij}}{r_{ij}} \right)^6 \right] \right. \\
 &\quad \left. + \frac{q_i q_j}{4\pi\epsilon_o} \left(\frac{1}{r_{ij}} + \frac{(\epsilon_s - 1)r_{ij}^2}{(2\epsilon_s + 1)r_c^3} \right) \right) \quad (1)
 \end{aligned}$$

where l_i , θ_i and ϕ_i denote bond length, bond angle and torsional angle, respectively, r_{ij} is the distance between interaction sites i and j and q_i is the partial charge on site i . Subscript o denotes parameter value at equilibrium. Flexible bonds are used and the potential energy of each bond is evaluated by using a simple harmonic potential (first-term on the rhs of equation (1)). Similarly, bond-angle fluctuations around the equilibrium angle are subject to harmonic fluctuations (second-term on the rhs of equation (1)). For all dihedral angles, a 3-fold symmetric torsional potential is used with $\phi = 0^\circ$ denoting a *trans* state (third-term on the rhs of equation (1)). Finally, non-bonded interactions are described by a LJ potential for van der Waals interactions while the reaction field model is used to account for the electrostatic interactions (last-term on rhs of equation (1); only for PDMS).

The reaction field method was preferred over the more widely used Ewald summation method because of its

computational efficiency. In equation (1), q_i and q_j are the partial charges of interaction sites i and j , ϵ_s is the dielectric constant of solvent, ϵ_o is the dielectric permittivity of vacuum (equal to $8.85419 \times 10^{-12} \text{ C}^2 \text{ J}^{-1} \text{ m}^{-1}$) and r_c is the cut-off distance for the electrostatic interactions. LJ and electrostatic interactions are calculated for all UAs on different chains and between UAs on the same chain that are three (four for the case of PDMS) or more bonds apart. Standard Lorentz–Berthelot combining rules are used to describe non-bonded LJ interactions between sites of different type:

$$\epsilon_{ij} = \sqrt{\epsilon_{ii}\epsilon_{jj}} \quad \text{and} \quad \sigma_{ij} = \frac{\sigma_{ii} + \sigma_{jj}}{2} \quad (2)$$

This force field was shown to predict accurately the PVT properties of polymer melts over a wide temperature and pressure range, solubility parameters and structural properties [12,13].

3. Molecular simulation details

All MD simulations were performed at the isobaric–isothermal (NPT) ensemble using the Nosé and Klein method [17–19]. In this case, the Lagrangian assumes the form:

$$\mathcal{L} = \sum_i \frac{m_i}{2} \dot{s}_i^2 - V_{\text{total}} + \frac{Q}{2} \dot{s}^2 - gk_B T \ln s + \frac{9}{2} WL^4 \dot{L}^2 - P_{\text{ext}} L^3 \quad (3)$$

where $g = 3nN_{\text{ch}} + 1$ is the number of degrees of freedom of the system, n is the number of atoms of each chain, N_{ch} is the number of chains, L is the box edge length, s is the “bath” degree of freedom used to control the temperature, W and Q are the inertia parameters associated with L and s , respectively, and P_{ext} is the externally set pressure. A fifth-order Gear predictor–corrector scheme is used to integrate the equations of motion in Cartesian coordinates. The values of the parameters W and Q are the same with those of previous work on PDMS [11].

All the polymer samples examined consisted of three chains of 80 monomer units. The initial configurations were obtained using the Cerius² software package of Accelrys Inc. and relaxed with molecular mechanics before MD [11,13]. MD simulations were performed with an integration time step of 0.5 fs to ensure system stability over time. The “equilibration” MD stage was 1 ns long, while the production run was 5 ns. In order to improve statistics in the calculated physical properties, for each state point several (four to six, depending on the conditions) runs were performed starting from different initial configurations. In each run, 5000 configurations were recorded at equal time intervals and they were used for the calculation of the thermodynamic and of the structural properties of polymer melt reported in Refs [12,13]. Furthermore, they were used for the evaluation

of the chemical potential of n -alkanes, n -perfluoroalkanes, noble and light gases in the polymer melts. Additional simulation details can be found in Refs [12,13].

The chemical potential was calculated using the Widom’s test particle insertion method [14]. According to this, one inserts a “ghost” molecule at a random position into the simulated system and calculates its interaction energy with the other molecules. This interaction energy is directly related to the excess chemical potential, μ^{ex} , of the “ghost” molecule. In the NPT ensemble, μ^{ex} is calculated by the expression:

$$\begin{aligned} \mu_{\text{ex}} &= \mu - \mu^{\text{ig}} \\ &= -\frac{1}{\beta} \ln \left[\frac{1}{\langle V \rangle_{NPT}} \left\langle V \left\langle \exp \left(-\beta U_{\text{ghost}}^{\text{intra}} - \beta U_{\text{ghost}}^{\text{inter}} \right) \right\rangle_{\text{Widom}} \right\rangle \right. \\ &\quad \left. \times \right]_{NPT} + \frac{1}{\beta} \ln \left\langle \exp \left(-\beta U_{\text{ghost}}^{\text{intra}} \right) \right\rangle_{\text{ideal gas}} \end{aligned} \quad (4)$$

where $\beta = 1/kT$, $U_{\text{ghost}}^{\text{inter}}$ is the intermolecular energy and $U_{\text{ghost}}^{\text{intra}}$ is the intramolecular energy of the “ghost” molecule. The latter is calculated independently in a single chain simulation. V is the instantaneous volume of the system and the brackets denote ensemble averaging over all configurations and spatial averaging over all “ghost” molecule positions. The UA force fields used to model n -alkanes (CH_4 to $n\text{-C}_6\text{H}_{14}$), n -perfluoroalkanes (CF_4 to $n\text{-C}_4\text{F}_{10}$), noble gases (He, Ne, Ar, Kr and Xe) and light gases (N_2 and O_2) are discussed in Ref. [13]. The fraction of successful “ghost” molecule insertions, that is insertions that do not result in major overlap with polymer molecules, decreases dramatically with the size of the “ghost” molecule. In figure 2, the fraction of successful insertions as a function of penetrant size parameter for spherical penetrants is shown at 300 and 450 K, for the case of PDMS. A similar picture is obtained for the other polymers, too. Obviously, for the heavier spherical and all

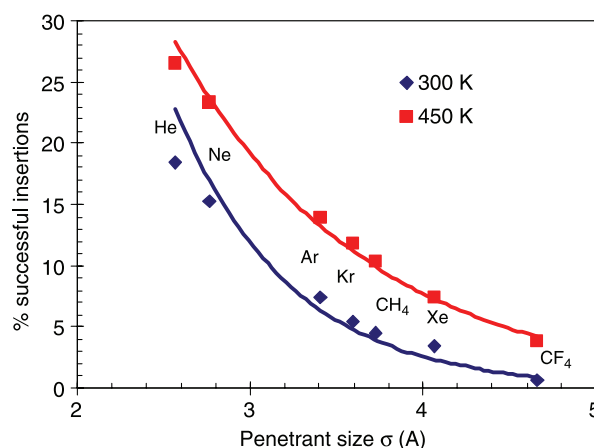


Figure 2. Percentage of successful insertions in PDMS as a function of penetrant size at 300 and 450 K. Each curve is an exponential fit to the corresponding simulation data.

Table 1. Simulation results for the infinite dilution solubility coefficient, S_o , of solutes in PDMSM.

Solute	S_o (cm^3 (STP)/ cm^3 pol atm)		
	300 (K)	350 (K)	400 (K)
CH ₄	0.21 ₁	0.20 ₁	0.19 ₁
C ₂ H ₆	1.21 ₈	0.83 ₄	0.58 ₁
C ₃ H ₈	3.5 ₁₀	2.1 ₁	1.06 ₂
<i>n</i> -C ₄ H ₁₀	18 ₇	4.8 ₃	2.07 ₃
<i>n</i> -C ₅ H ₁₂	56 ₃₆	9 ₄	3.9 ₃
<i>n</i> -C ₆ H ₁₄	171 ₉₇	24 ₁₂	5.8 ₄
He	0.032 ₁	0.046 ₁	0.061 ₁
Ne	0.043 ₁	0.056 ₁	0.070 ₁
Ar	0.147 ₉	0.145 ₁	0.146 ₁
Kr	0.428 ₄	0.378 ₇	0.323 ₁
Xe	1.37 ₈	0.99 ₅	0.690 ₁
N ₂	0.06 ₁	0.07 ₁	0.08 ₁
O ₂	0.10 ₁	0.11 ₁	0.11 ₁

Subscripts denote statistical uncertainty in the last significant figure as calculated in simulation, for example, 0.21₁ corresponds to 0.21 ± 0.01 .

non-spherical penetrants, this fraction is small and a large number of insertions are needed for statistically reliable simulations.

From the excess chemical potential, one may calculate the Henry's law constant of a solute (gas or solvent) in polymer, according to the expression:

$$H_{\text{solute} \rightarrow \text{pol}} = \lim_{x_{\text{solute}} \rightarrow 0} \left(\frac{\rho_{\text{pol}}}{\beta} \exp(\beta \mu_{\text{solute}}^{\text{ex}}) \right) \quad (5)$$

where ρ_{pol} is the density of the polymer. Alternatively, the solubility coefficient, S_o at infinite dilution can be calculated from the expression:

$$S_o = \frac{22,400 \text{ cm}^3(\text{STP})/\text{mol}}{\text{RT}} \lim_{x_{\text{solute}} \rightarrow 0} \exp(-\beta \mu_{\text{solute}}^{\text{ex}}) \quad (6)$$

In this work, calculations are reported in terms of S_o in units of $\text{cm}^3(\text{STP})/(\text{cm}^3 \text{ pol atm})$ that are used widely in membrane science and technology. STP corresponds to an absolute pressure of 101.325 kPa and a temperature of 273.15 K. Molecular simulation results are reported in tables 1–4.

Table 2. Simulation results for the infinite dilution solubility coefficient, S_o , of solutes in PDMSTM.

Solute	S_o (cm^3 (STP)/ cm^3 pol atm)		
	300 (K)	350 (K)	400 (K)
CH ₄	0.42 ₂	0.38 ₁	0.36 ₁
C ₂ H ₆	2.33 ₂	1.5 ₁	1.05 ₁
C ₃ H ₈	6.3 ₆	3.9 ₂	2.08 ₂
<i>n</i> -C ₄ H ₁₀	23 ₄	9.4 ₃	4.06 ₅
<i>n</i> -C ₅ H ₁₂	79 ₁₁	18 ₄	7.7 ₂
<i>n</i> -C ₆ H ₁₄	219 ₃₅	38 ₁₅	14.8 ₅
He	0.060 ₁	0.080 ₁	0.110 ₁
Ne	0.079 ₁	0.102 ₁	0.127 ₁
Ar	0.274 ₁	0.276 ₃	0.273 ₁
Kr	0.856 ₁	0.66 ₁	0.57 ₁
Xe	2.7 ₁	1.62 ₉	1.21 ₂
N ₂	0.12 ₁	0.13 ₂	0.15 ₁
O ₂	0.20 ₁	0.21 ₁	0.22 ₁

Table 3. Simulation results for the infinite dilution solubility coefficient, S_o , of solutes in poly(DMSM–*alt*-DMSTM).

Solute	S_o (cm^3 (STP)/ cm^3 pol atm)		
	300 (K)	350 (K)	400 (K)
CH ₄	0.34 ₁	0.29 ₂	0.27 ₁
C ₂ H ₆	2.13 ₁₃	1.2 ₁	0.85 ₅
C ₃ H ₈	5.4 ₄	2.9 ₄	1.6 ₂
<i>n</i> -C ₄ H ₁₀	17 ₆	7 ₁	3.2 ₃
<i>n</i> -C ₅ H ₁₂	47 ₂₂	15 ₁	6 ₁
<i>n</i> -C ₆ H ₁₄	163 ₈₉	41 ₁	12 ₃
He	0.050 ₁	0.066 ₁	0.085 ₁
Ne	0.063 ₁	0.080 ₁	0.096 ₁
Ar	0.19 ₁	0.22 ₂	0.21 ₁
Kr	0.63 ₄	0.52 ₃	0.45 ₁
Xe	1.9 ₃	1.32 ₇	0.97 ₆
N ₂	0.095 ₃	0.102 ₄	0.116 ₄
O ₂	0.16 ₂	0.16 ₁	0.16 ₁

4. Simplified PC-SAFT

The simplified PC-SAFT equation of state, developed by von Solms *et al.* [20], is a simplified version of PC-SAFT [5]. The two models are identical for pure compounds and the only difference lies in the mixing rules. PC-SAFT is expressed in terms of the reduced Helmholtz energy as:

$$\tilde{a} = \frac{A}{k\text{TN}} = \tilde{a}^{\text{id}} + \tilde{a}^{\text{hc}} + \tilde{a}^{\text{disp}} + \tilde{a}^{\text{assoc}} \quad (7)$$

where \tilde{a}^{id} is the ideal gas contribution, \tilde{a}^{hc} is the contribution of the hard-sphere chain reference systems, \tilde{a}^{disp} is the dispersion contribution arising from the square-well attractive potential, and \tilde{a}^{assoc} is the contribution due to association (not used here, since all systems examined are non-associating). The expressions for the contributions from the ideal gas and dispersion are identical to those of Gross and Sadowski [5], and the reader is referred to their paper for more detail. The contribution to the hard-chain

Table 4. Simulation results for the infinite dilution solubility coefficient, S_o , of solutes in PDMS.

Solute	S_o (cm^3 (STP)/ cm^3 pol atm)		
	300 (K)	375 (K)	450 (K)
CH ₄	0.47 ₁	0.36 ₁	0.33 ₁
C ₂ H ₆	2.6 ₁	1.15 ₃	0.75 ₁
C ₃ H ₈	7.1 ₄	2.36 ₃	1.22 ₁
<i>n</i> -C ₄ H ₁₀	21 ₂	4.9 ₄	1.98 ₁
<i>n</i> -C ₅ H ₁₂	62 ₁₄	9.1 ₄	3.1 ₁
<i>n</i> -C ₆ H ₁₄	191 ₈₆	19 ₁	4.8 ₁
CF ₄	0.28 ₆	0.20 ₁	0.21 ₁
C ₂ F ₆	0.35 ₁	0.24 ₁	0.21 ₁
C ₃ F ₈	0.97 ₁	0.37 ₂	0.34 ₁
<i>n</i> -C ₄ F ₁₀	2.6 ₄	0.9 ₁	0.58 ₂
He	0.058 ₁	0.091 ₁	0.125 ₁
Ne	0.078 ₁	0.109 ₁	0.139 ₁
Ar	0.31 ₂	0.27 ₁	0.26 ₁
Kr	0.76 ₄	0.58 ₂	0.47 ₂
Xe	2.8 ₂	1.4 ₁	0.9 ₁
N ₂	0.15 ₁	0.15 ₁	0.16 ₁
O ₂	0.22 ₁	0.21 ₁	0.19 ₁

Table 5. sPC-SAFT parameters for various compounds examined here. The temperature range of experimental data and the percentage AAD for saturated liquid density and vapour pressure are shown.

Compound	MW (g/mol)	m (–)	σ (Å)	ε/k (K)	T (K)	AAD (ρ/P^{sat}) (%)
Ne	20.2	1.000	2.7874	33.94	22–40	2.27/5.22
Kr	83.8	0.9610	3.6634	167.26	110–185	0.52/0.40
Xe	131.3	0.9025	4.0892	239.69	148–260	0.97/0.56
O ₂	32.0	1.1217	3.2098	114.96	55–154	0.32/0.18
CF ₄	88.0	2.1779	3.1383	122.65	115–205	0.16/0.18
C ₂ F ₆	138.0	2.7543	3.3459	141.69	160–260	0.54/1.23
C ₃ F ₈	188.0	3.4547	3.3031	154.20	180–305	0.20/1.48
C ₄ F ₁₀	238.0	3.8326	3.5361	162.28	195–340	0.70/0.38
PDMSM	10000	563.00	3.8054	272.40	–	–
PDMS	1540	49.9730	3.5310	204.95	298–343	–

Parameters for additional compounds can be found in Ref. [15].

term is made up of two contributions: the hard-sphere term and the chain term, so that:

$$\tilde{a}^{hc} = \tilde{m}\tilde{a}^{hs} - \sum_i x_i(m_i - 1) \ln g_{ii}^{hs}(d_i^+) \quad (8)$$

where \tilde{m} is a mean segment length defined simply as $\tilde{m} = \sum_i x_i m_i$ and the hard-sphere term is given by:

$$\tilde{a}^{hs} = \frac{4\eta - 3\eta^2}{(1 - \eta)^2} \quad (9)$$

Here, x_i is the mole fraction of component i . The radial distribution function of the hard-sphere fluid at contact is:

$$g^{hs}(d^+) = \frac{1 - (\eta/2)}{(1 - \eta)^3} \quad (10)$$

The volume fraction $\eta = \pi \rho \tilde{m} d^3 / 6$ is based on the diameter of an equivalent one-component mixture:

$$d = \left(\frac{\sum_i x_i m_i d_i^3}{\sum_i x_i m_i} \right)^{1/3} \quad (11)$$

where the individual d_i are temperature-dependent segment diameters:

$$d_i = \sigma_i \left[1 - 0.12 \exp\left(-3 \frac{\varepsilon_i}{kT}\right) \right] \quad (12)$$

Thus, it is assumed that all the segments in the mixture have a mean diameter d , which gives a mixture volume fraction identical to that of the actual mixture.

For non-associating small molecules and polymers, the model has three characteristic parameters, that are the segment number m (for polymers, a more convenient way is to use m/MW), the temperature-independent segment diameter σ , and the segment interaction energy ε/k . For small molecules, these parameters are usually fitted to experimental vapor pressure and liquid density data over a wide subcritical temperature range. In this work, model parameters for non-polymers were either regressed here and are shown in table 5, or taken from Ref. [15]. Polymers, however, have a non-measurable vapour pressure and an alternative approach is needed. A large number of approaches have been proposed so far for

SAFT-based models [5,6,16] that each seems to work well for specific cases only. In this work, sPC-SAFT calculations were performed for PDMSM and PDMS mixtures only, since for the other polymers experimental melt density data were very limited.

PDMSM is a non-polar elastomer whose chemical structure resembles closely the structure of polyolefins. Consequently, energetic interactions between PDMSM segments are expected to be close to those between polyolefin segments. For this reason, the ε/k value proposed previously for polyethylene [16] was used also for PDMSM. The other two parameters were fitted to the relatively few melt density data available for over a narrow temperature and pressure range and are shown in table 5 [11]. With these parameters, the percentage average absolute deviation (% AAD) between experimental melt density data or accurate simulation calculations [11] in the temperature range 300–400 K and pressure up to 160 MPa, that are considered within less than 0.2% from experiment, and sPC-SAFT correlation is on the order of 1%.

PDMS is a widely studied polymer and so melt density data are available over an extensive temperature and pressure range [21]. In this case, all three sPC-SAFT were fitted to PDMS melt density and the values are shown in table 5. With this parameter set, the % AAD between experimental data and model correlation is 0.1%.

Extension to mixtures requires combining rules for segment energy and diameter. The Lorentz–Berthelot rule shown in equation (2) is employed for the macroscopic calculations too. For mixtures where experimental data are available, an energy interaction parameter, k_{ij} , is often used as a correction to the geometric mean rule.

5. Results and discussion

5.1 Molecular simulation results for infinite dilution solubility coefficients

For PDMSM, PDMSTM and their copolymer, simulation results for S_0 at 300, 350 and 400 K are reported in tables 1–3, while for PDMS calculations over a wider temperature range up to 450 K are provided in table 4.

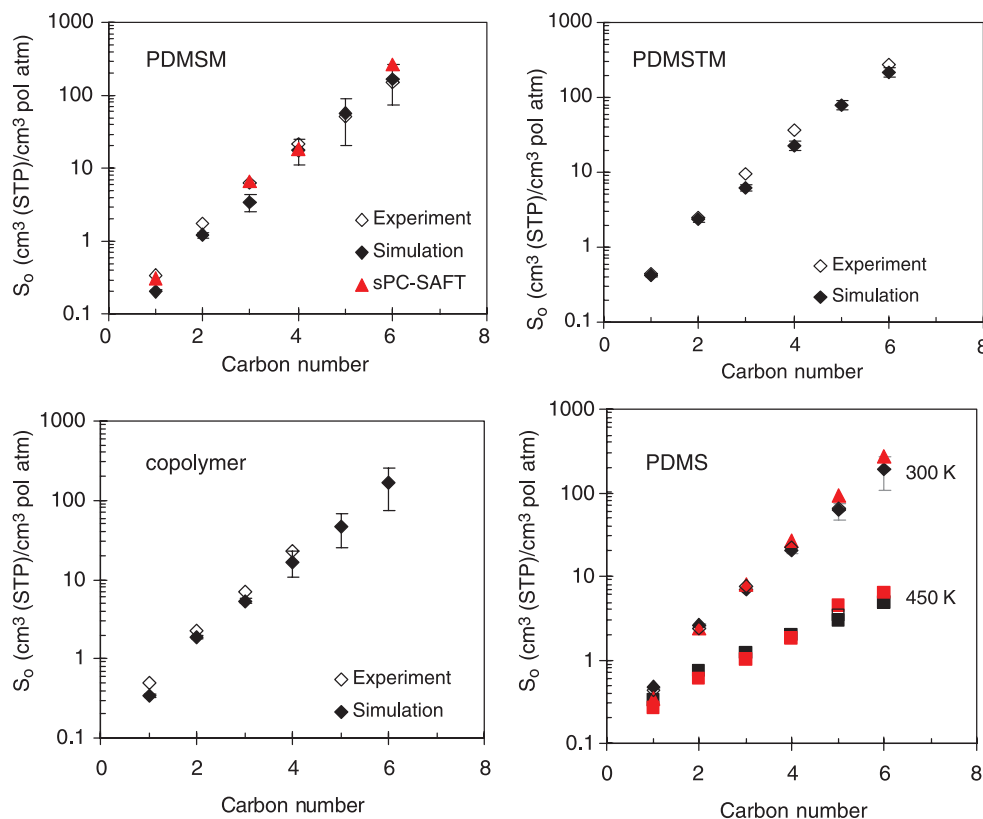


Figure 3. Experimental data (open points), molecular simulation predictions (diamonds) and sPC-SAFT predictions (triangles) for the infinite dilution solubility coefficient of *n*-alkanes in PDMSM, PDMSTM, copolymer and PDMS at 300 K and 0.1 MPa. For PDMS, an experimental point at 423 K and simulation (black squares) and sPC-SAFT (grey squares; red in online version) predictions at 450 K are shown also.

Selected results are discussed here in detail, mainly for systems where experimental data are available. Calculations and limited experimental data for S_0 of *n*-alkanes in PDMSM, PDMSTM, copolymer and PDMS at 300 K and 0.1 MPa are shown in figure 3. In all cases, solubility increases with *n*-alkane carbon number. Simulation results are in very good agreement with experiment, when available. Furthermore for a given *n*-alkane, S_0 values are very similar for the various polymers. In other words, the chemical structure of these polymers has very little effect on the solubility of the solutes.

S_0 of various solutes in a polymer correlate very nicely with the solute experimental critical temperature [22]. In figure 4, experimental data [22], molecular simulation calculations and simplified PC-SAFT predictions are shown for eight different gases in PDMS. Predictions from both models are in very good agreement with the experimental data in all cases. For the case of He, where the deviation between experiment and simulation assumes the highest value, additional experimental data exist in the literature that are closer to the simulation value [13].

In figure 5, simulation results for S_0 of some of the relatively lighter solutes examined here (from lower to higher T_c , results are shown for He, Ne, N_2 , O_2 and Kr) in various polymers are shown at 300 K. For He and Ne, S_0 values for each one of them are very similar for the various polymers. However, for the heavier of the components

shown, significant differences are progressively observed for S_0 in the various polymers for a given solute.

An interesting temperature dependence on S_0 is observed for different solutes. For the lighter gases that include He and Ne, solubility increases with temperature. For the intermediate gases including Ar, N_2 and O_2 , solubility is relatively independent of temperature, while for the heavier ones such as CH_4 , Kr, Xe, CF_4 and beyond

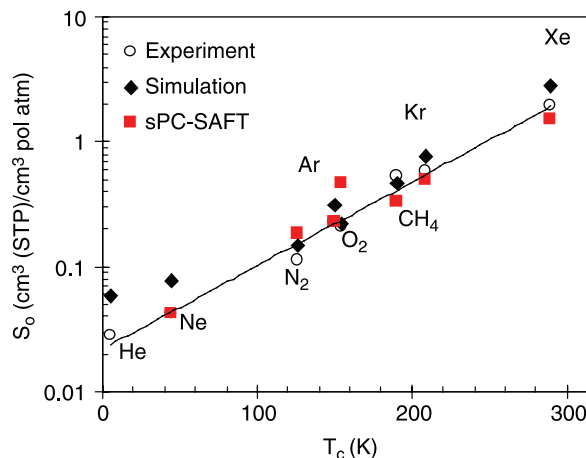


Figure 4. Experimental data (circles) [22], molecular simulation (diamonds) and simplified PC-SAFT (squares) predictions for S_0 of gases in PDMS at 300 K. The solid line is a fit to experimental data.

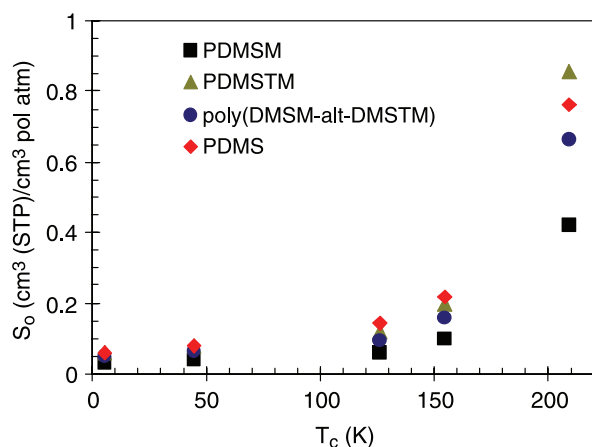


Figure 5. Molecular simulation predictions for S_o of light components in various polymers at 300 K as a function of light component experimental critical temperature.

solubility decreases as temperature increases. In figure 6, S_o values for the various gases in PDMS as a function of temperature are shown verifying this argument. An alternative way to present these data is shown in figure 7 where S_o at different temperatures is shown as a function of solute critical temperature for PDMSM and PDMS.

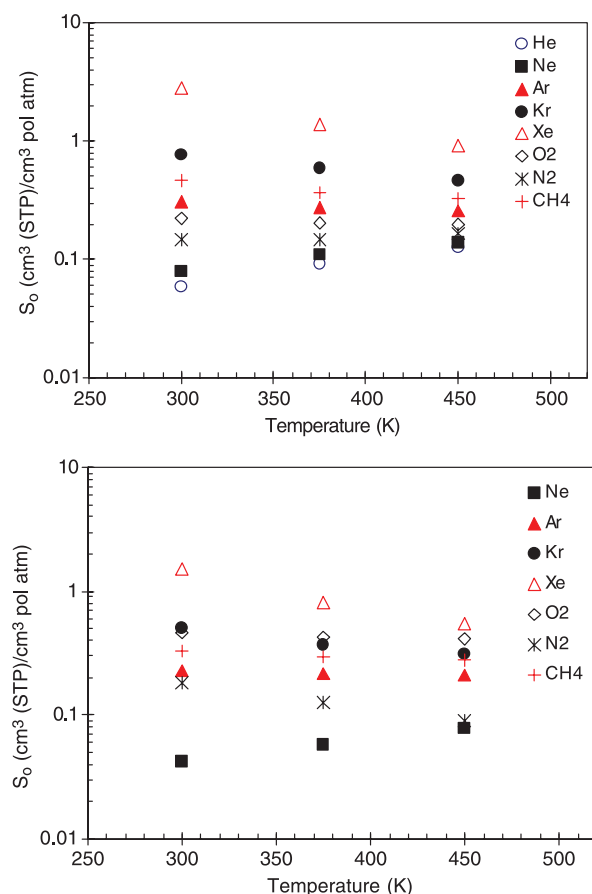


Figure 6. Molecular simulation predictions (top) and sPC-SAFT predictions (bottom) for S_o of He, Ne, Ar, Kr, Xe, O_2 , N_2 and CH_4 in PDMS at 300, 375 and 450 K.

The plots for PDMSTM and the copolymer are very similar to PDMSM and are not shown. A systematic crossover is observed in all cases. For PDMSM, PDMSTM and the copolymer the crossover temperature is estimated from a least square fit to the data and is around 150–160 K while for PDMS it is a little lower, at around 125–135 K.

This behaviour has been observed experimentally by van Amerongen [23] for various gases in natural rubber where the crossover was estimated to occur between N_2 and O_2 , in the critical temperature range of $T_c = 126$ –154 K. Furthermore, the same phenomenon was predicted by Curro *et al.* [24] for noble gases in polyethylene using an accurate integral equation theory known as polymer reference interaction site model (PRISM). PRISM predicted a crossover value of $T_c = 65$ K which is in reasonable agreement with experiments and predictions shown here considering the approximations assumed in PRISM theory. With the exception of prediction from PRISM, all other sets of data/calculations agree in the temperature range of crossover. In other words, the crossover temperature seems to be independent on the nature of the polymer (at least for the polymers examined) and depends only on the solute.

A phenomenological explanation for this behaviour can be based on combined energetic and entropic effects. A temperature increase results in a decrease of the polymer density or increase of the free volume accessible to small molecules and so light gases become more soluble. On the other hand, the temperature increase makes heavier solute molecules behave more like gas molecules with a significant decrease in their density and substantial decrease in their solubility in polymer.

5.2 Macroscopic modelling of infinite dilution and finite solute concentration properties

sPC-SAFT was used to calculate the infinite dilution solubility coefficient and the entire isotherm of various PDMSM–solvent and PDMS–solvent mixtures. A small temperature independent interaction parameter, k_{ij} , was used for some mixtures and was regressed from experimental isotherm data. The only exception was the polymer–methane mixture, where a temperature-dependent k_{ij} was needed for accurate correlation of the data. In figure 8, experimental data and sPC-SAFT correlations are shown for PDMSM–methane ($k_{ij} = -0.19$ at 283 K, -0.18 at 303 K and -0.15 at 323 K) and PDMSM–propane ($k_{ij} = -0.085$). Additional calculations were performed for PDMSM–*n*-butane at 295.15 K ($k_{ij} = -0.014$) and PDMSM–*n*-hexane at 298.15 K ($k_{ij} = -0.07$). In all cases, sPC-SAFT provides accurate correlation of the data. The k_{ij} values fitted to these phase equilibrium data were used subsequently to predict the S_o values for the various mixtures, as shown in figure 3 (top left). Macroscopic model predictions agree very well with experimental data and molecular simulation predictions discussed above.

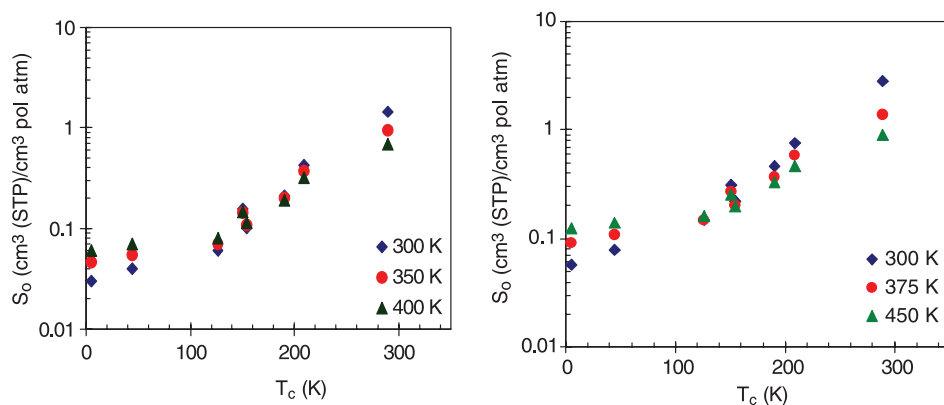


Figure 7. Molecular simulation predictions for S_o of He, Ne, Ar, Kr, Xe, O₂, N₂ and CH₄ in (left) PDMSM at 300, 350 and 400 K, and (right) PDMS at 300, 375 and 450 K, as a function of solute critical temperature.

For the case of PDMS mixtures, sPC-SAFT predicts accurately S_o of *n*-alkanes at 300 K and of *n*-pentane at 363 and 423 K without any binary parameter adjustment. Calculations are shown in figure 3 (bottom right). Furthermore, in figure 9 sPC-SAFT predictions are shown for three PDMS–*n*-pentane isotherms over a wide composition range. These results manifest that

properly selected pure polymer parameter values can result in accurate prediction of mixture phase equilibria. For the case of polar hydrocarbon solvents, a small k_{ij} value is needed so that the model correlates experimental data accurately. In figure 10, PDMS–toluene experimental data [1] and sPC-SAFT calculations with $k_{ij} = 0.015$ are shown at two different temperatures. Agreement is very good again. Calculations with $k_{ij} = 0.0$ are shown also for comparison.

sPC-SAFT provides also accurate prediction of the solubility of gases in PDMS. Calculations are shown in figure 4 and agree very well with the experimental data and molecular simulation results. He-containing mixtures were not modeled with sPC-SAFT since the model does not account for the quantum effects that are important for He, even at high temperatures. S_o for all gases examined with sPC-SAFT with the exception of Ne exhibit negative temperature dependence, as shown in figure 6 (bottom). These results indicate that sPC-SAFT predictions are in closer agreement with PRISM theory that predicts a critical temperature crossover for the solubility at 65 K,

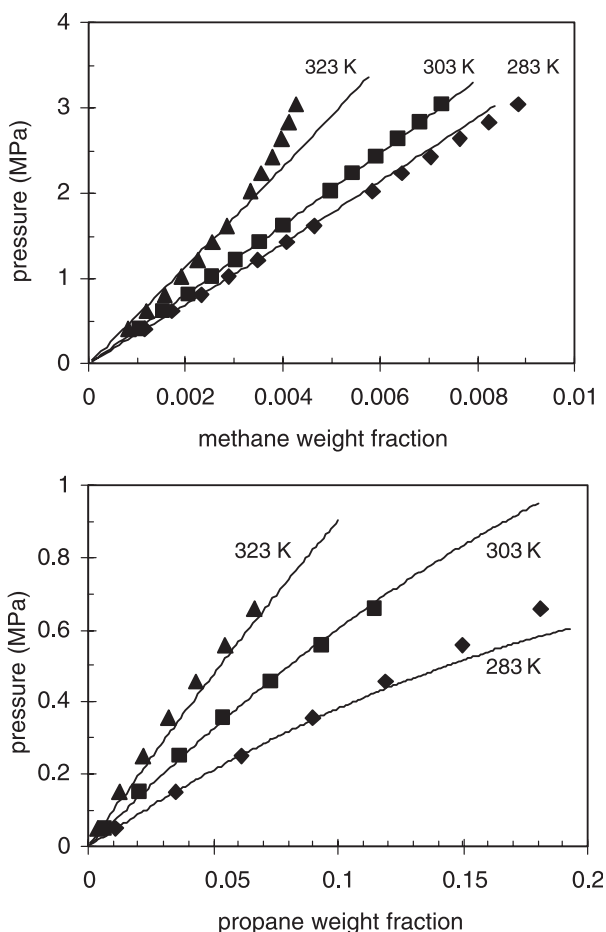


Figure 8. Experimental data (points) [25] and sPC-SAFT correlation of (top) methane solubility in PDMSM and (bottom) propane solubility in PDMSM.

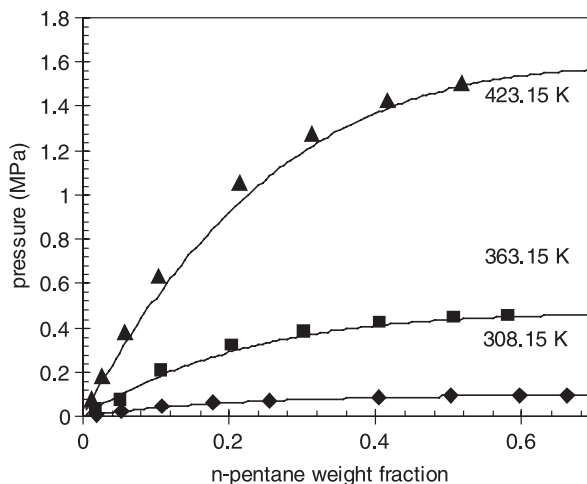


Figure 9. PDMS–*n*-pentane phase equilibria at 308.15, 363.15 and 423.15 K. Experimental data (points) [26], and sPC-SAFT prediction (solid curves; $k_{ij} = 0.0$).

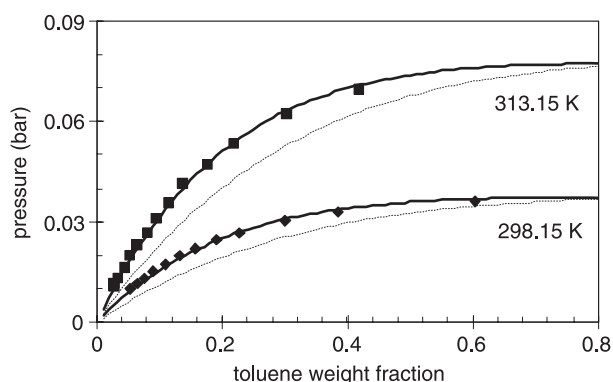


Figure 10. PDMS-toluene phase equilibria at 298.15 and 313.15 K. Experimental data (points), and simplified PC-SAFT prediction (thin curves; $k_{ij} = 0.0$) and correlation (thick curves; $k_{ij} = 0.015$).

as explained above, and not with molecular simulation or experimental data for natural rubber. Such behaviour requires further investigation.

6. Conclusions

Molecular simulation using realistic molecular models and macroscopic models with strong statistical mechanics basis are reliable tools for the accurate calculation of solute solubility in polymers over a wide temperature and composition range. In this work, molecular simulation was shown to predict accurately the solubility of various organic components and gases in four silicon-containing polymers while sPC-SAFT provided accurate prediction of PDMS-solute mixture infinite dilution properties and phase equilibria over a wide composition range. For the case of PDMSM—*n*-alkane mixtures, a small temperature-independent (with the exception of methane) and composition-independent binary interaction parameter was needed. For a given solute and temperature, the solubility in the four polymers examined was similar, as predicted by molecular simulation. Finally, the temperature dependence of the solubility is a strong function of the solute as predicted by molecular simulation, going from positive for light gases to negative for heavier components, and rather independent of the polymer nature. sPC-SAFT predicts a systematic decrease of the solubility with temperature for all gases but Ne (calculations for He were not performed) in agreement with polymer integral equation theory predictions.

Acknowledgements

Research in Greece is supported by the European Union—European Social Fund, the Greek Secretariat of Research and Technology and Bayer Technology Services GmbH. We are thankful to the Danish Research Council of Technology and Production Sciences for financial support in the form of a visiting professorship to IGE under the

project: *Development and Validation of Computational Tools for soft Material Structure and Properties*. Dr John G. Curro of Sandia National Laboratories is gratefully acknowledged for helpful comments regarding the solubility crossover phenomenon.

References

- [1] W. Hao, H.S. Elbro, P. Alessi. *Polymer Solution Data Collection. DECHEMA Chemistry Data Series, Volume XIV*, Dechema, Frankfurt am Main (1992).
- [2] J.M. Prausnitz, R.N. Lichtenthaler, E.G. de Azevedo. *Molecular Thermodynamics of Fluid-Phase Equilibria*, 3rd ed., Prentice-Hall, Englewood Cliffs, NJ (1998).
- [3] H.S. Huang, M. Radosz. Equation of state for small, large, polydisperse and associating molecules. *Ind. Eng. Chem. Res.*, **29**, 2284 (1990).
- [4] S.-J. Chen, I.G. Economou, M. Radosz. Density-tuned polyolefin phase equilibria. 2. Multicomponent solutions of alternating poly(ethylene-propylene) in subcritical and supercritical olefins. Experiment and SAFT model. *Macromolecules*, **25**, 4987 (1992).
- [5] J. Gross, G. Sadowski. Modeling polymer systems using the Perturbed-Chain Statistical Associating Fluid Theory equation of state. *Ind. Eng. Chem. Res.*, **41**, 1084 (2002).
- [6] T. Lindvig, I.G. Economou, R.P. Danner, M.L. Michelsen, G.M. Kontogeorgis. Modeling of multicomponent vapor-liquid equilibria for polymer-solvent systems. *Fluid Phase Equilib.*, **220**, 11 (2004).
- [7] C.G. Panayiotou. Lattice fluid theory of polymer solutions. *Macromolecules*, **20**, 861 (1987).
- [8] I.C. Sanchez, C.G. Panayiotou. Equations of state thermodynamics of polymer and related solutions. In *Models for Thermodynamic and Phase Equilibria Calculations*, S. Sandler (Ed.), Dekker, New York (1994).
- [9] S.K. Nath, B.J. Banaszak, J.J. de Pablo. Simulation of ternary mixtures of ethylene, 1-hexene, and polyethylene. *Macromolecules*, **34**, 7841 (2001).
- [10] I.G. Economou. Molecular simulation of phase equilibria for industrial applications. In *Computer Aided Property Estimation for Process and Product Design*, G.M. Kontogeorgis, R. Gani (Eds.), pp. 279–307, Elsevier Science B.V., Dordrecht (2004).
- [11] V.E. Raptis, I.G. Economou, D.N. Theodorou, J. Petrou, J.H. Petropoulos. Molecular dynamics simulation of structure and thermodynamic properties of poly(dimethylsilamethylene) and hydrocarbon solubility therein: toward the development of novel membrane materials for hydrocarbon separation. *Macromolecules*, **37**, 1102 (2004).
- [12] Z.A. Makrodimitri, V.E. Raptis, I.G. Economou. Molecular dynamics simulation of structure, thermodynamic and transport properties of poly(dimethylsilamethylene), poly(dimethylsilatri-methylene) and their alternating copolymer. *J. Phys. Chem. B*, **110**, 16047 (2006).
- [13] Z.A. Makrodimitri, R. Dohrn, I.G. Economou. Atomistic simulation of poly(dimethylsiloxane): force field development, structure and thermodynamic properties of polymer melt and solubility of *n*-alkanes, *n*-perfluoroalkanes, noble and light gases. *Macromolecules*, **40**, 1720 (2007).
- [14] B. Widom. Some topics in the theory of fluids. *J. Chem. Phys.*, **39**, 2808 (1963).
- [15] A. Tihic, G.M. Kontogeorgis, N. von Solms, M.L. Michelsen. Applications of the simplified perturbed-chain SAFT equation of state using an extended parameter table. *Fluid Phase Equilib.*, **248**, 29 (2006).
- [16] I.A. Kouskoumvekaki, N. von Solms, T. Lindvig, M.L. Michelsen, G.M. Kontogeorgis. Novel method for estimating pure-component parameters for polymers: application to the PC-SAFT equation of state. *Ind. Eng. Chem. Res.*, **43**, 2830 (2004).
- [17] S. Nosé, M.L. Klein. Constant pressure molecular-dynamics for molecular systems. *Mol. Phys.*, **50**, 1055 (1983).
- [18] S. Nosé. A unified formulation of the constant temperature molecular-dynamics methods. *J. Chem. Phys.*, **81**, 511 (1984).
- [19] S. Nosé. A molecular-dynamics method for simulations in the canonical ensemble. *Mol. Phys.*, **52**, 255 (1984).

- [20] N. von Solms, M.L. Michelsen, G.M. Kontogeorgis. Computational and physical performance of a modified PC-SAFT equation of state for highly asymmetric and associating mixtures. *Ind. Eng. Chem. Res.*, **42**, 1098 (2003).
- [21] P.A. Rodgers. Pressure volume temperature relationships for polymeric liquids—a review of equations of state and their characteristic parameters for 56 polymers. *J. Appl. Polym. Sci.*, **48**, 1061 (1993).
- [22] Y. Kamiya, Y. Naito, K. Terada, K. Mizoguchi, A. Tsuboi. *Macromolecules*, **33**, 3111 (2000).
- [23] G.J. van Amerongen. *Rub. Chem. Technol.*, **37**, 1065 (1964).
- [24] J.G. Curro, K.G. Honnell, J.D. McCoy. Theory for the solubility of gases in polymers: application to monatomic solutes. *Macromolecules*, **30**, 145 (1997).
- [25] V.M. Shan, B.J. Hardy, S.A. Stern. Solubility of carbon dioxide, methane and propane in silicone polymers—effect of polymer backbone chains. *J. Polym. Sci. Polym. Phys.*, **31**, 313 (1993).
- [26] O. Pfohl, C. Riebesell, R. Dohrn. Measurement and calculation of phase equilibria in the system *n*-pentane + poly(dimethylsiloxane) at 308.15–423.15 K. *Fluid Phase Equilib.*, **202**, 289 (2002).